Dynamic Influence of the Two Membrane-Proximal Immunoglobulin-Like Domains upon the Peptide-Binding Platform Domain in Class I and Class II Major Histocompatibility Complexes: Normal Mode Analysis

Hiroyuki Nojima,[a,#] Kazuhiko Kanou,[a,#] Kenshu Kamiya,[b] Koichiro Atsuda,[a] Hideaki Umeyama,[a] and Mayuko Takeda-Shitaka*,[a]

[a] *School of Pharmacy, Kitasato University; 5–9–1 Shirokane, Minato-ku, Tokyo 108–8641, Japan: and* [b] *School of Science, Kitasato University; 1–15–1 Sagamihara, Kanagawa 228–8555, Japan.*

Received March 12, 2009; accepted August 9, 2009; published online August 25, 2009

Major histocompatibility complexes (MHCs) mainly fall into class I and class II. The two classes have similar structures, with two membrane-proximal immunoglobulin-like domains and a peptide-binding platform domain, though their organizations are different. We simulated the dynamics of a whole and partial model deficient in either of the two membrane-proximal domains for class I and class II using normal mode analysis. Our study showed that the influence of the two membrane-proximal domains upon the dynamics of the platform domain were decisively different between class II and class I. Both membrane-proximal domains (the α2 and β2 domains) of class II MHC, especially the α2 domain, influenced the most important pocket that accommodates a large hydrophobic anchor side chain of the N-terminal side of the bound peptide, though the pocket was not in the α2 domain neighborhood. By contrast, the two membrane-proximal domains (the α3 and β_2m domains) of class I MHC had little influence upon the most important pocket that accommodates the N-terminal residue of the bound peptide. These results suggest that the two membrane-proximal domains of class II MHC have a greater influence upon peptide-binding than those of class I MHC.

Key words major histocompatibility complex; class I; class II; membrane-proximal immunoglobulin-like domain; peptide-binding platform domain; normal mode analysis

Major histocompatibility complexes (MHCs) are cell-surface glycoproteins that play an important role in immune response against infection. MHCs bind to a small peptide derived from either host or pathogen proteins, and present them to a T cell as a part of the immune system's mechanism for identifying and responding to foreign antigens. The engagement of an MHC molecule with a peptide by an antigen receptor on a cell causes the stimulation of the T cell and the activation of the immune response. The striking characteristic of MHCs is their ability to bind to various peptides in order to ensure an immune response against many possible pathogens.

MHCs mainly fall into class I and class II. Class I MHC is composed of a heavy chain and a β_2-immunoglobulin (β_2m). The heavy chain is divided into three domains, α1, α2 and α3. The α1 and α2 domains are also functionally expressed as a peptide-binding platform domain, as the two domains are complicatedly intertwined. The platform domain forms an eight-stranded β-sheet and two α-helical regions, and a bound peptide is accommodated between the two α-helical regions on the β-sheet (Fig. 1A).[1] The α3 and β_2m domains are known as the membrane-proximal immunoglobulin-like domains because they are located between the platform domain and the cell surface.

Conversely, class II MHC is composed of two asymmetric chains, the α- and β-chains, divided into the α1 and α2 domains, and the β1 and β2 domains, respectively. Thus the α1 and β1 domains come from different chains, but the two domains are also functionally expressed as a peptide-binding platform domain, because they are complicatedly intertwined. Surprisingly, the platform, β2 and α2 domains of class II MHC are very similar in structure to the platform, α3 and β_2m domains of class I MHC, respectively (Figs. 1A, B).[2,3] However, there is a difference in peptide-binding between both classes: Class I MHC binds to the peptide limited in length, usually 8—10 residues,[4—6] while class II MHC binds to the peptide without apparent restriction in length (*ca.* 8—23 amino acids in length).[7,8]

Previous studies concerning MHCs were interested in the crystal structure of the platform domain required for peptide-binding and presenting to T cells.[1—9] Moreover, some experimental and theoretical studies of the peptide-free platform domain have received attention because its structure has not yet been crystallized in both classes.[10—20] On the other hand, the two membrane-proximal domains have attracted less interest than the platform domain. Some biochemical studies investigated the two membrane-proximal domains of class I MHC, suggesting the importance of β_2m in peptide-binding.[21,22] However, there are no experimental or theoretical studies concerning the two membrane-proximal domains of class II MHC.

In this study, we simulated the dynamics of a whole and partial model deficient in either of the two membrane-proximal domains for class I and class II using normal mode analysis, and compared the influence of the two membrane-proximal domains upon the dynamics of the platform domain between both classes. Our study suggests that the two membrane-proximal domains of class II MHC have a greater influence upon the most important peptide-binding pocket than those of class I MHC.

Experimental

Models Used for Normal Mode Analysis Initial atomic coordinates were taken from X-ray crystallographic structures stored in the Brookhaven Protein Data Bank (PDB). A structure of human leukocyte antigen (HLA)-

* To whom correspondence should be addressed. e-mail: shitakam@pharm.kitasato-u.ac.jp
# These authors contributed equally to this work.

Table 1. Domain Structures of Each Model and Summaries of Energy-Optimization and Normal Mode Calculations

		"Class I" models			"Class II" models		
		"α3-removed"	"β_2m-removed"	"Whole"	"β2-removed"	"α2-removed"	"Whole"
Platform domain		α1 (G h[a)]1—N h86)+α2 (Q h87—R h181)			α1 (E α3—Y α79)+β1 (T β3—Q β92)		
Membrane-proximal domains[b)]		—	α3 (T h182—E h275)	α3	—	β2 (R β93—A β190)	β2
		β_2m (M β_2[c)]0—M $\beta_2$99)	—	β_2m	α2 (T α80—A α182)	—	α2
Bound peptide		RT (I309—V317)	RT	RT	HA (P306—T318)	HA	HA
Total number of residues		290	284	384	283	278	381
RMSD[d)]	*vs.* the initial coordinates[e)]	1.90—2.03	2.01—2.28	2.07—2.25	2.21—2.45	1.97—2.46	1.82—1.96
	between the six energy-optimized structures[f)]	0.53—1.11	0.72—1.18	0.47—1.18	0.67—1.59	0.71—1.44	0.65—1.05
Number of modes	Total	1289	1224	1674	1227	1224	1632
	$<$50 cm^{-1} [g)]	219—227	211—225	293—303	230—241	213—234	301—317
	($<$50 cm^{-1}/total) (%)	17.0—17.6	17.2—18.4	17.5—18.1	18.7—19.6	17.4—19.1	18.4—19.4

a) "h" means the heavy chain. *b*) The β2 and α2 domains of class II MHC structurally correspond to the α3 and β_2m domains of class I MHC, respectively. *c*) "β_2" means β_2m. *d*) RMSD was calculated for all atoms except for hydrogen. *e*) RMSD was calculated between the initial coordinates and the six energy-optimized structures. *f*) RMSD was calculated between the six energy-optimized structures. *g*) Number of modes $<$50 cm^{-1} have a range because distributions of normal modes are slightly different between the six energy-optimized structures.

A2 with a peptide derived from human immunodeficiency virus (HIV) reverse transcriptase [9 residues: RT309—317 (ILKEPVHGV)] was adopted as the "class I" model, (PDB code: 1HHJ).[6)] In the PDB, an A-chain (the heavy chain) of 275 residues (the α1, α2 and α3 domains, G h1—E h275), a B-chain (β_2m) of 100 residues (M $\beta_2$0—M $\beta_2$99) and a C-chain (RT peptide) of 9 residues were used as the "class I whole" model. A part of the A-chain (the α1 and α2 domains, G h1—R h181), the B- and C-chains were used as the "class I α3-removed" model, while the A- and C-chains were used as the "class I β_2m-removed" model.

A structure of HLA-DR1 with a peptide derived from influenza virus hemagglutinin [13 residues: HA306—318 (PKYVKQNTLKLAT)] was adopted as the "class II" model (PDB code: 1DLH).[3)] In the PDB, a D-chain (α-chain) of 180 residues (the α1 and α2 domains, E α3—A α182), an E-chain (β-chain) of 188 residues (the β1 and β2 domains, T β3—A β190) and an F-chain (HA peptide) of 13 residues were used as the "class II whole" model. The D-chain, a part of the E-chain (the β1 domain, T β3—Q β92) and the F-chain were used as the "class II β2-removed" model, while a part of the D-chain (the α1 domain, E α3—Y α79), and the E- and F-chains were used as the "class II α2-removed" model.

The details of domain structure for each model are shown in Table 1.

Energy Optimization Each model was energetically optimized to obtain structures for normal mode analysis. In the energy optimization, bond length, bond angle and dihedral angle were treated as parameters.[23)] To lower computational cost in the energy optimization process, we adopted a slightly modified Assisted Model Building with Energy Refinement (AMBER) united atom-force field. In this field, aliphatic and aromatic carbon-bonded hydrogen atoms were neglected, and, instead, the three suspected carbon atoms whose atomic weights were 13.02, 14.03 and 15.03, respectively, were introduced.[24,25)] "Slight modification" means that bond-angle and dihedral-angle were neglected in the parameters of a disulfide bond, and the "suspected potential" in which the distance between two S atoms was treated as only a parameter was introduced.[23)] The validity of the simplified force field has been illustrated in our previous study.[26)]

A distance-dependent dielectric constant (r/Å) for electrostatic energy was used to consider short-distance electrostatic interactions.[27)] Position-restriction energy, E, expressed in Eq. 1 was imposed in the energy optimization process.

$$E = \sum_{i}^{N} K(r_i - r_i^0)^2 \quad (1)$$

In Eq. 1, K (kcal/mol Å) is a force constant, and r_i and r_i^0 are displaced and initial coordinates of the ith atom, respectively. The above restriction was gradually relaxed by decreasing the K value so that normal mode analysis could be executed near the initial coordinates. Some energy-optimized structures were prepared from the initial coordinates of a model using different relaxation patterns.[15,16,26,28—30)] All the obtained energy-optimized structures, however, do not have an energy minimum accurate enough to approximate to a harmonic potential. Therefore, we examined the normal modes calculated using the obtained energy-optimized structures, and omitted the energy-optimized structures improper to normal mode analysis. After all, six proper energy-optimized structures were sampled for a model. Root mean square deviation (RMSD) between the six energy-optimized structures and the initial coordinates (for all atoms except hydrogen atoms) ranged from 1.82 to 2.46 Å in all models, indicating that the energy-optimized structures are near the initial coordinates (Table 1).

Normal Mode Analysis Normal mode analysis was performed using programs developed by our laboratory.[23)] In the normal mode calculation, only dihedral angle was treated as a parameter. A RMS fluctuation at the ith Cα atom, F_i, was calculated by Eq. 2[31)]:

$$\langle F_i^2 \rangle = \langle \Delta r_i^2 \rangle = k_B T \sum_k (|\mathbf{a}_{ki}|^2 / \omega_k^2) \quad (2)$$

in which $\mathbf{a}_{ki}$ is a projection vector of the kth normal mode with frequency ω_k on the Cartesian components of displacement vector $\Delta\mathbf{r}_i$, k_B is the Bolzmann constant, and T is the absolute temperature. The fluctuation was calculated by our program, assuming a temperature of 300 K, and was then determined by averaging the data of its six sampled energy-optimized structures.[15,16,26,28—30)]

When attention is focused on the motion of a component, it can be broken down into internal and external motions.[32)] Eckart's condition was applied to extract the internal motion of a component (for example, a domain) from the whole motion.[33)] A "significant fluctuation difference" was calculated be-

tween two models by Wilcoxon's rank sum test, a nonparametric test (significance level 2.5%), using data of the six energy-optimized structures for each model.[15,16,26,28,29] If a fluctuation difference at a Cα atom was significant between two models, it was expressed as a "significant fluctuation difference" by subtracting the averages of the two models. If not, it was expressed as zero.

Generally, the dynamic characteristic of a large molecule is heavily influenced by low frequency modes.[27,31,34—36] In this study, the fluctuation was expressed in the low frequency modes ($<50\,cm^{-1}$), as there were little differences from expression in all-frequency modes (data not shown). A number of the low frequency modes shared 17.0—19.6% of all frequency modes in all models (Table 1).

Results

The Fluctuation Differences between the "Class I Whole" and "Class I α3-Removed" Models, and between the "Class II Whole" and "Class II β2-Removed" Models

The α3 domain of class I MHC structurally corresponds to the β2 domain of class II MHC, as shown in Fig. 1. Thus, the fluctuation difference between "class I whole" and "class I α3-removed" models was compared with that between the "class II whole" and "class II β2-removed" models. The fluctuations of the "class I α3-removed" (Fig. 2A) and "class II β2-removed" (Fig. 2B) models were superimposed on those of the "class I whole" and "class II whole" models, respectively. The fluctuation of each model was expressed by the internal motion of either the platform or another proximal domain. At a Cα atom, a "significant fluctuation difference" was calculated between the "whole" and "removed" models (yellow lines in Fig. 2), while a "remarkable fluctuation difference" (less than -0.03) was noted in the platform domain (the red lines and red vertical shadows under these lines in Fig. 2).

Comparing between the "class I whole" and "class I α3-removed" models, ten residues showed a "remarkable fluctuation difference" (residues h29—30 and h49 in the α1 domain, and h105—108, h176—177 and h180 in the α2 domain; Fig. 2A). The "class I" models have two important pockets to accommodate the N-terminal (I RT309, the "N-terminal side" pocket) and C-terminal (V RT317, the "C-terminal side" pocket) residues of the bound peptide.[6] The "N-terminal side" pocket is composed of residues h7, h59, h63 and h66 in the α1 domain and h159, h167 and h171 in the α2 domain (the red circles in Fig. 2A), while the "C-terminal

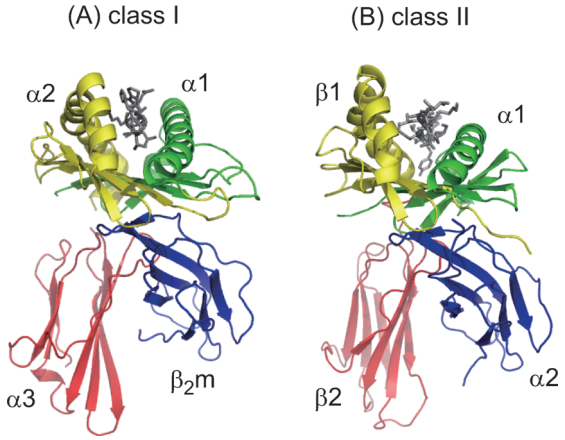

Fig. 1. Schematic Structures of (A) Class I (PDB Code, 1HHJ) and (B) Class II (PDB Code, 1DLH) MHCs Separated by Color for Each Domain

Class I MHC is divided into the α1 (green), α2 (yellow) and α3 (red) domains and β_2-immunoglobulin (β_2m, blue). Class II MHC is divided into the α1 (green), α2 (blue), β1 (yellow) and β2 (red) domains. The bound peptides are indicated by gray sticks. The α1, α2 and α3 domains and β_2m in class I MHC are similar in secondary structure to the α1, β1, β2 and α2 domains in class II MHC, respectively.

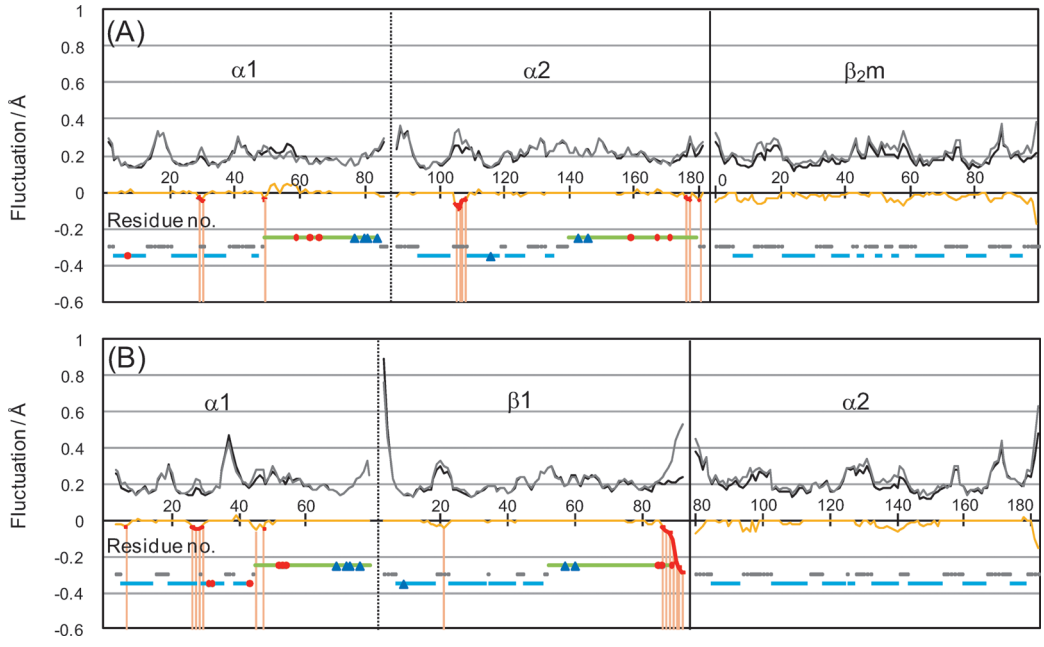

Fig. 2. Cα Atom RMS Fluctuations of (A) the "Class I Whole" and "Class I α3-Removed" Models and of (B) the "Class II Whole" and "Class II β2-Removed" Models

In each figure, the fluctuation of the "removed" model (gray line) is superimposed on that of the "whole" model (black line). The "significant fluctuation difference" between the "removed" and "whole" models is indicated in a yellow line. The "significant fluctuation difference" less than -0.03 is colored red as a "remarkable fluctuation difference" and shadowed by light red vertical line under the red line. The notations of secondary structure, α-helical region, β-strand and loop are shown at the bottom by light green, light blue and gray bars, respectively. In (A), the residues forming two pockets to accommodate the N-terminal (I 309) and C-terminal (V317) residues of RT peptide are marked by red circles and blue triangles, respectively. In (B), the residues forming two pockets to accommodate two hydrophobic anchor side chains in the N-terminal (Y308) and C-terminal (L316) sides of HA peptide are marked by a red circle and a blue triangle, respectively.

side" pocket is composed of residues h77, h80—81 and h84 in the α1 domain and h116, h143 and h146 in the α2 domain (the blue triangles in Fig. 2A). These residues, however, did not show a "remarkable fluctuation difference."

By contrast, comparing between the "class II whole" and "class II β2-removed" models, fifteen residues showed a "remarkable fluctuation difference" (residues α6, α26—29, α45 and α47 in the α1 domain, and β21, β86—92 in the β1 domain, Fig. 2B). The "class II" models have no pockets to accommodate both terminal residues of the bound peptide because they stick out from the platform domain. To compensate for this, the "class II" models have two important deep pockets to accommodate two large hydrophobic anchor side chains of the N-terminal side (Y HA308, the "N-terminal side" pocket) and the C-terminal side (L HA316, the "C-terminal side" pocket) of the bound peptide.[3] The "N-terminal side" pocket is composed of residues α31, α32, α43 and α52—54 in the α1 domain and β86 and β89 in the β1 domain (the red circles in Fig. 2B), while the "C-terminal side" pocket is composed of residues α69, α72, α73 and α76 in the α1 domain and β9, β57 and β60 in the β1 domain (the blue triangles in Fig. 2B). Among these residues, G β86 and F β89, which participate in the formation of the "N-terminal side" pocket, showed a "remarkable fluctuation difference."

The Fluctuation Differences between the "Class I Whole" and "Class I β_2m-Removed" Models, and between the "Class II Whole" and "Class II α2-Removed" Models β_2m of class I MHC structurally corresponds to the α2 domain of class II MHC, as shown in Fig. 1. Thus, the fluctuation difference between the "class I whole" and "class I β_2m-removed" models was compared with that between the "class II whole" and "class II α2-removed" models. The fluctuations of the "class I β_2m-removed" (Fig. 3A) and "class II α2-removed" (Fig. 3B) models were superimposed on those of the "class I whole" and "class II whole" models, respectively. The fluctuation of each model was expressed by the internal motion of either the platform or another proximal domain. A "significant fluctuation difference" and "remarkable fluctuation difference" were determined between two models in the same manner described in the preceding paragraph.

Thirty-three residues showed a "remarkable fluctuation difference" when comparing the "class I whole" and "class I β_2m-removed" models (residues h10—12, h14—18 and h49—50 in the α1 domain, and h93—94, h105—108, h115, h117—123 and h173—181 in the α2 domain, Fig. 3A). The residues were larger in number than those found between the "class I whole" and "class I α3-removed" models (ten residues), suggesting that, in class I MHC, β_2m has an influence upon a larger extent of the platform domain than the α3 domain. However, when the "N-terminal side" and "C-terminal side" pockets were investigated (the red circles and blue triangles in Fig. 3A), there were no residues that showed a "remarkable fluctuation difference" (Fig. 3A).

By contrast, 43 residues showed a "remarkable fluctuation difference" when the "class II whole" and "class II α2-removed" models were compared (residues α14—17, α24—31, α33—36, α38, α40, α42—47, α50, α75, α77 and α79 in the α1 domain, and β3, β5—8, β33—35, β37, β86—89 and β91—92 in the β1 domain; Fig. 3B). The residues were larger in number than those found between the "class II whole" and "class II β2-removed" models (fifteen residues), suggesting that, in the "class II" models as well as the "class I" models, the α2 domain has an influence upon a larger extent of the platform domain than the β2 domain. When the "N-terminal side" and "C-terminal side" pockets were studied (the red circles and blue triangles in Fig. 3B), residues I α31, W α43, G β86 and F β89, which participate in the formation of the "N-terminal side" pocket, showed a "remarkable fluctuation difference" (Fig. 3B).

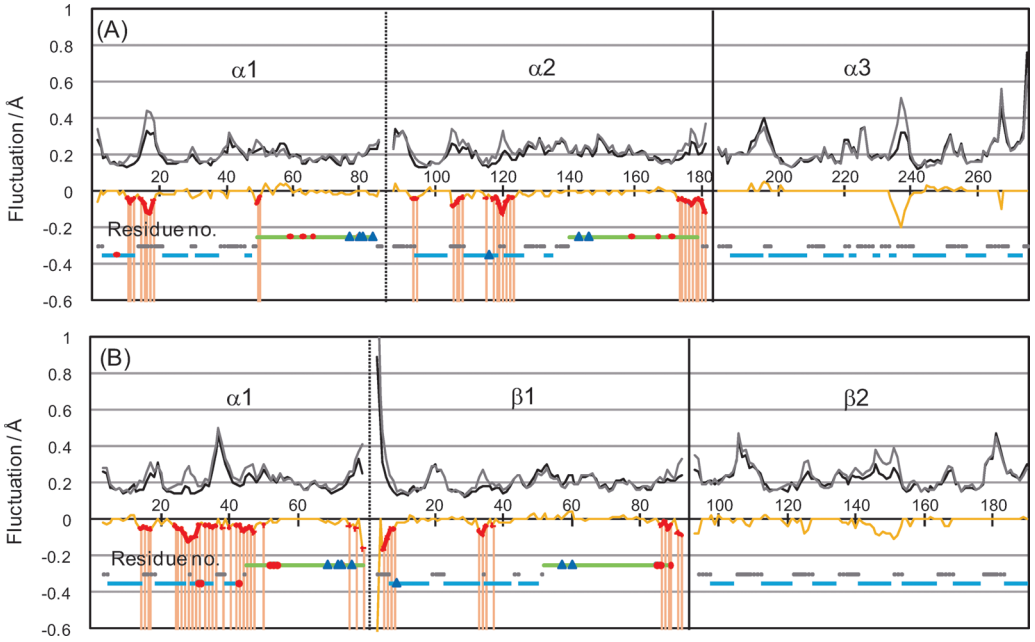

Fig. 3. Cα Atom RMS Fluctuations of (A) the "Class I Whole" and "Class I β_2m-Removed" Models and of (B) the "Class II Whole" and "Class II α2-Removed" Models

The notations of fluctuations, secondary structures and peptide-binding pockets are shown in the same manner as Fig. 2.

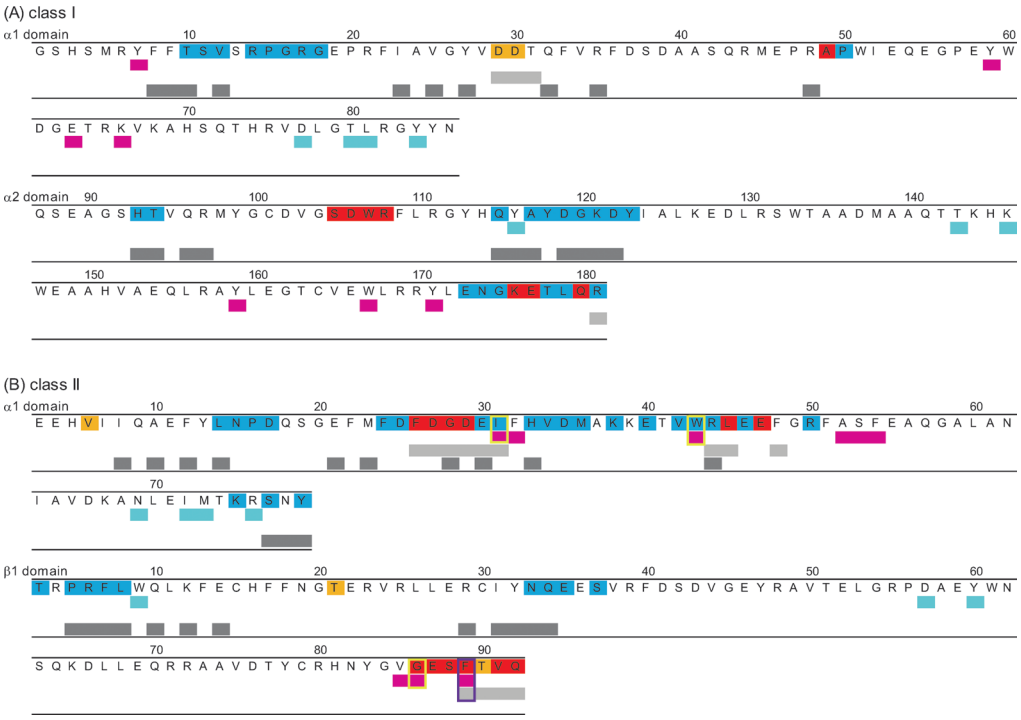

Fig. 4. Relationship between "Remarkable Fluctuation Difference" and the Short Contact in the (A) "Class I" and (B) "Class II" Models

In each figure, the "remarkable fluctuation difference" found only between the "class I whole" (or "class II whole") and "class I α3-removed" (or "class II β2-removed") models is marked on the amino acid sequence in orange. The "remarkable fluctuation difference" found only between the "class I whole" (or "class II whole") and "class I β_2m-removed" (or "class II α2-removed") models is marked on the amino acid sequence in blue. The "remarkable fluctuation difference" found between the "class I whole" (or "class II whole") model and both the "class I removed" (or "class II removed") models is marked on the amino acid sequence in red. The important peptide-binding pockets that accommodate the "N-terminal" (magenta) and "C-terminal" (cyan) sides of the bound peptide, as shown in Fig. 2, are marked on the second top line. The short contact of the platform domain with the α3 domain (or the β2 domain) and β_2m (or the α2 domain) is marked on the third top line in light gray and the bottom line in dark gray, respectively. The short contact was defined as occurring where the distance between residues is less than 4 Å.

The Short Contact of the Two Membrane-Proximal Domains with the Platform Domain If a domain is removed from a molecule, the residue which is in the removed domain neighborhood generally undergoes a fluctuation change. In both classes, however, the residues of the two membrane-proximal domain neighborhoods (less than 4 Å, the light and dark gray marks in Fig. 4) were not always in agreement with the residues which showed a "remarkable fluctuation difference." The "N-terminal side" and "C-terminal side" pockets were then studied in both classes (magenta and cyan marks in Fig. 4). In the "class I" models, only one residue, Y h116 was in the β_2m neighborhood but did not show a "remarkable fluctuation difference" between the "class I whole" and "class I β_2m-removed" models. In the "class II" models, only one residue, F β89 which showed a "remarkable fluctuation difference" between the "class II whole" and "class II β2-removed" models, was in the β2 domain neighborhood (the purple frame in Fig. 4B). I α31 was in the β2 domain neighborhood, but did not show a "remarkable fluctuation difference" between the "class II whole" and "class II β2-removed" models. I α31, W α43, G β86 and F β89 showed a "remarkable fluctuation difference" between the "class II whole" and "class II α2-removed" models, but none of the four residues were in the α2 domain neighborhood (the purple and yellow frames in Fig. 4B). Thus, the "N-terminal side" pocket of class II MHC is influenced by the α2 domain, though it is not in the α2 domain neighborhood.

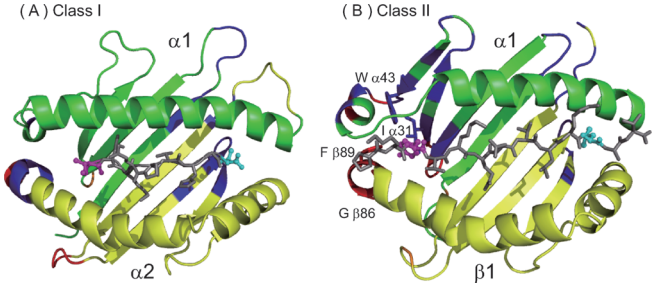

Fig. 5. Schematic Structures of the Peptide-Binding Platform Domains of the (A) "Class I" and (B) "Class II" Models

The domains and peptides are colored as for Fig. 1. In (A), the N-terminal (I309) and C-terminal (V317) residues of RT peptide are colored purple and cyan, respectively. In (B), two residues with a hydrophobic anchor side chain in the N-terminal (Y308) and C-terminal (L316) sides of HA peptide are colored purple and cyan, respectively. In each figure, the "remarkable fluctuation difference" found only between the "class I whole" (or class II whole") and "class I α3-removed" (or "class II β2-removed") models is marked on the structure in orange. The "remarkable fluctuation difference" found only between the "class I whole" ("class II whole") and "class I β_2m-removed" (or "class II α2-removed") models is marked on the structure in blue. The "remarkable fluctuation difference" found between the "class I whole" ("class II whole") model and both the "class I removed" (or "class II removed") models is marked on the structure in red. The residues which participate in the formation of the important peptide-binding pockets, and showed a "remarkable fluctuation difference," are marked with the side chain.

Discussion

As a complementary theoretical tool, molecular dynamics has been shown to be a powerful approach for the study of fluctuations on the nanosecond time scale.[31] Recently, the molecular dynamics simulation on the peptide-class I MHC complex *vs.* the isolated platform domain was performed and

found that the two membrane-proximal domains (the α3 and β_2m domain) cannot be neglected in peptide-binding stability of the platform domain.[37] This study, however, could not classify the contribution difference between the α3 and β_2m domain influence upon the platform domain. A limited time scale with available computational capability makes the molecular dynamics simulation on the interdomain interaction in a large molecule difficult. To avoid this problem, we selected normal mode analysis that has less computational cost than molecular dynamics. However, if two models are compared by normal mode analysis based on only one energy-optimized structure for each model, it is incontrovertible that the result contains a trivial computational artifact. To omit such a problem, we adopted six energy-optimized structures for a model. As shown in Table 1, RMSD between the sampled energy-optimized structures ranged from 0.47 to 1.59 Å in all models. This range did not deviate greatly from the range of RMSD between the X-ray crystal structures of class I MHC homologues whose sequence is identical (from 0.09 to 1.74 Å) and the range of RMSD between the X-ray crystal structures of class II MHC homologues whose sequence is identical (from 0.09 to 1.40 Å), indicating that the energy-optimized structures varied moderately. Our previous studies have inferred the statistical comparison between two models using six energy-optimized structures for each model.[15,16,26,28,29] For example, the "significant fluctuation difference" between two models was calculated by the non-parametric Wilcoxon's rank sum test. Statistical analysis convinces us that our studies are not guided based on trivial computational artifact.

We attempted to detect the difference between the influence that class I and class II two membrane-proximal domains have upon the dynamics of the platform domain. The "remarkable fluctuation differences" found between the "whole" model and the "removed" models are conclusively illustrated in Fig. 5. The membrane-proximal domains of the "class I" models little influenced the important peptide-binding pockets (Fig. 5A). On the other hand, both the membrane-proximal domains of the "class II" models, especially the α2 domain influenced major parts (I α31, W α43, G β86 and F β89) of the "N-terminal side" pocket (Fig. 5B), but, as shown in Fig. 4, these residues were not in the α2 domain neighborhood. In both the classes, the "N-terminal side" pocket is more important in peptide-binding than the "C-terminal side" pocket. For example, in class I MHC, the N-terminus of a bound peptide is accommodated in the "N-terminal side" pocket without exception, but the C-terminus of a bound peptide is not always accommodated in the "C-terminal side" pocket.[38] In class II MHC, some experimental and computational studies indicated that the introduction of a short peptide composed of two residues or G β86Y substitution to occupy only the "N-terminal side" pocket induced a significant stabilization of not only the pocket but also of the whole peptide-binding groove.[14,18,20] The other computational studies discussed the peptide-free form of class II MHC and demonstrated the flexibility of the "N-terminal side" pocket and its importance in peptide-binding over the other pockets.[16,19] Considering these circumstances, our results suggest that the membrane-proximal domains of class II MHC have a greater influence upon peptide-binding than those of class I MHC. Such results are probably attributed to the peptide-binding manner of each class. The "N-terminal side" pocket of class I MHC is located on the inside of the platform domain, and composed of structurally stable α-helices and β-strands (Fig. 5A). On the other hand, compared with the former, the "N-terminal side" pocket of class II MHC is located on an edge of the platform domain, and composed of a flexible loop (α31 and α32) and a connecting region (from β86 to β92) between the second α-helices and the β2 domain (Fig. 5B). Such a flexibility of the "N-terminal side" pocket might make the pocket sensitive to the two membrane-proximal domains, though it is not in the α2 domain neighborhood. In addition, the delicate cooperation of the two membrane-proximal domains with the "N-terminal side" pocket might permit class II MHC to bind to bound peptides without apparent restriction on length (*ca.* 8—23 amino acids in length).

In this study, we adopted HLA-DR1 as a simulation target of class II MHC. To examine whether our results using HLA-DR1 showed a major characteristic of class II MHC homologues registered up to this point, the conservation of the residues in the platform domain was investigated by Position-Specific Iterated Basic Local Alignment Search Tool (PSI-BLAST).[39] In the α1 domain, 70.0% of the residues which showed a "remarkable fluctuation difference" between the "class II whole" model and either of the two "class II removed" models (20 residues in 29 residues), were the most conserved amino acids among class II MHC homologues. This percentages was higher than those of the other residues in the α1 domain (60.4%, 29 residues in 48 residues). In addition, all the residues which showed a "remarkable fluctuation difference" between the "class II whole" model and both the "class II removed" models (6 residues) were the most conserved amino acids among class II MHC homologues. On the other hand, in the β1 domain, 88.2% of the residues which showed a "remarkable fluctuation difference" between the "class II whole" model and either of the two "class II removed" models (15 residues in 17 residues), were the most conserved amino acids among class II MHC homologues. This percentage was a little higher than those of the other residues in the β1 domain (84.9%, 62 residues in 73 residues). In addition, all the residues which showed a "remarkable fluctuation difference" between the "class II whole" model and both the "class II removed" models (6 residues), were the most conserved amino acids among class II MHC homologues. We investigated the conservation of the most important pocket of class II MHC, the "N-terminal side" pocket, in detail. In HLA-DR1, I α31, W α43, G β86 and F β89 showed a "remarkable fluctuation difference" and were major in forming the "N-terminal side" pocket. In these residues, Wα43, G β86 and F β89 were conserved by 50%, 23% and 73% of class II homologues, respectively. The conservation percentage of G β86 (23%) was not high, but all of the three residues were the most conserved amino acids among class II MHC homologues. I α31 (with a conservation percentage of 12%) was not highly conserved among class II MHC homologues. However, the total conservation percentage of similar character amino acids (V, L, I and M) was 73% in class II MHC homologues. These results, therefore, demonstrate that our findings are not limited to HLA-DR1 only but are a major characteristic of class II MHC homologues.

In conclusion, our study showed that the influence of the two membrane-proximal domains upon the dynamics of the platform domain were decisively different between class II and class I. Both membrane-proximal domains (the α2 and β2 domains) of class II MHC, especially the α2 domain, influenced the most important peptide-binding pocket, the "N-terminal side" pocket, though the pocket was not in the α2 domain neighborhood. By contrast, the two membrane-proximal domains (the α3 and β_2m domains) of class I MHC had little influence on the "N-terminal side" pocket. These results suggest that the two membrane-proximal domains of class II MHC have a greater influence upon peptide-binding than those of class I MHC.

References

1) Bjorkman P. J., Saper M. A., Samraoui B., Bennett W. S., Strominger J. L., Wiley D. C., *Nature* (London), **329**, 506—512 (1987).
2) Brown J. H., Jardetzky T. S., Gorga J. C., Stern L. J., Urban R. G., Strominger J. L., Wiley D. C., *Nature* (London), **364**, 33—39 (1993).
3) Stern L. J., Brown J. H., Jardetzky T. S., Gorga J. C., Urban R. G., Strominger J. L., Wiley D. C., *Nature* (London), **368**, 215—221 (1994).
4) Zhang W., Young A. C., Imarai M., Nathenson S. G., Sacchettini J. C., *Proc. Natl. Acad. Sci. U.S.A.*, **89**, 8403—8407 (1992).
5) Fremont D. H., Stura E. A., Matsumura M., Peterson P. A., Wilson I. A., *Science*, **257**, 919—927 (1992).
6) Madden D. R., Garboczi D. N., Wiley D. C., *Cell*, **75**, 693—708 (1993).
7) Chicz R. M., Urban R. G., Lane W. S., Gorga J. C., Stern L. J., Vignali D. A., Strominger J. L., *Nature* (London), **358**, 764—768 (1992).
8) Rudensky A., Perston-Hurlburt P., Hong S. C., Barlow A., Janeway C. A., Jr, *Nature* (London), **353**, 622—627 (1991).
9) Utz U., Koenig S., Coligan J. E., Biddison W. E., *J. Immunol.*, **149**, 214—221 (1992).
10) Meng W. S., von Grafenstein H., Haworth I. S., *Int. Immunol.*, **9**, 1339—1349 (1997).
11) Bouvier M., Wiley D. C., *Nat. Struct. Biol.*, **5**, 377—384 (1998).
12) Hansen T., *Nat. Struct. Biol.*, **5**, 340—341 (1998).
13) Meng W. S., von Grafenstein H., Haworth I. S., *Int. Immunol.*, **12**, 949—957 (2000).
14) Sato A. K., Zarutskie J. A., Rushe M. M., Lomakin A., Natarajan S. K., Sadegh-Nasseri S., Benedek G. B., Stern L. J., *J. Biol. Chem.*, **275**, 2165—21732 (2000).
15) Nojima H., Takeda-Shitaka M., Kurihara Y., Adachi M., Yoneda S., Kamiya K., Umeyama H., *Chem. Pharm. Bull.*, **50**, 1209—1214 (2002).
16) Nojima H., Takeda-Shitaka M., Kurihara Y., Kamiya K., Umeyama H., *Chem. Pharm. Bull.*, **51**, 923—928 (2003).
17) Zacharias M., Springer S., *Biophys. J.*, **87**, 2203—2214 (2004).
18) Gupta S., Höpner S., Rupp B., Günther S., Dickhaut K., Agarwal N., Cardoso M. C., Kühne R., Wiesmüller K. H., Jung G., Falk K., Rötzschke O., PLoS ONE 2008;3:e1814.
19) Painter C. A., Cruz A., López G. E., Stern L. J., Zavala-Ruiz Z., PLoS ONE. 2008;3:e2403.
20) Yaneva R., Springer S., Zacharias. M., *Biopolymers*, **91**, 14—27 (2009).
21) Vitiello A., Potter T. A., Sherman L. A., *Science*, **250**, 1423—1426 (1990).
22) Cook J. R., Myers N. B., Hansen T. H., *J. Immunol.*, **157**, 2256—2261 (1996).
23) Kamiya K., Sugawara Y., Umeyama H., *J. Comput. Chem.*, **24**, 826—841 (2003).
24) Weiner S. J., Kollman P. A., Case D. A., Singh U. C., Ghio C., Alagona G., Profeta S. J., Weiner P., *J. Am. Chem. Soc.*, **106**, 765—784 (1984).
25) Weiner S. J., Kollman P. A., Nguyen D. T., Case D. A., *J. Comput. Chem.*, **107**, 230—252 (1986).
26) Nojima H., Takeda-Shitaka M., Kanou K., Kamiya K., Umeyama H., *Chem. Pharm. Bull.*, **56**, 635—641 (2008).
27) Jääskeläinen S., Verma C. S., Hubbard R. E., Linko P., Caves L. S., *Protein Sci.*, **7**, 1359—1367 (1998).
28) Adachi M., Kurihara Y., Nojima H., Takeda-Shitaka M., Kamiya K., Umeyama H., *Protein Sci.*, **12**, 2125—2131 (2003).
29) Kurihara Y., Watanabe T., Nojima H., Takeda-Shitaka M., Kamiya K., Umeyama H., *Chem. Pharm. Bull.*, **51**, 754—758 (2003).
30) Takeda-Shitaka M., Nojima H., Takaya D., Kanou K., Iwadate M., Umeyama H., *Chem. Pharm. Bull.*, **52**, 643—645 (2004).
31) Brooks B., Karplus M., *Proc. Natl. Acad. Sci. U.S.A.*, **80**, 6571—6575 (1983).
32) Ishida H., Jochi Y., Kidera A., *Proteins*, **32**, 324—333 (1998).
33) Eckart C., *Phys. Rev.*, **47**, 552—558 (1935).
34) Go N., Noguti T., Nishikawa T., *Proc. Natl. Acad. Sci. U.S.A.*, **80**, 3696—3670 (1983).
35) Levitt M., Sander C., Stern P. S., *J. Mol. Biol.*, **181**, 423—447 (1985).
36) Nishikawa T., Go N., *Proteins*, **2**, 308—329 (1987).
37) Wan S., Coveney P., Flower D. R., *J. Comput. Chem.*, **25**, 1803—1813 (2004).
38) Collins E. J., Garboczi D. N., Wiley D. C., *Nature* (London), **371**, 626—629 (1994).
39) Altschul S. F., Madden T. L., Schäffer A. A., Zhang J., Zhang Z., Miller W., Lipman D. J., *Nucleic Acids Res.*, **25**, 3389—3402 (1997).